Fizika Nizkikh Temperatur, 2000, v. 26, Nos. 9/10, p. 981–991

Infrared and EPR spectroscopic study of open-shell reactive intermediates: F + NH_3 in solid argon

Eugenii Ya. Misochko, Ilya U. Goldschleger, and Alexander V. Akimov

Institute of Problems of Chemical Physics of the Russian Academy of Sciences
142432 Chernogolovka, Moscow district, Russia
E-mail: ilya@icp.ac.ru

Charles A. Wight

Department of Chemistry, University of Utah, Salt Lake City, Utah 84112, USA

Received February 1, 2000

Mobile F atoms react with NH_3 molecules in an argon matrix at temperatures $T = 7–35$ K. The open-shell NH_2–HF complex was observed by EPR and infrared spectroscopies as the main product of this reaction. The hyperfine constants of the NH_2–HF complex $a_N = 1.20$ mT, $a_H = 2.40$ mT, and $a_F = 0.70$ mT were determined from the EPR spectra of samples using NH_3, $^{15}NH_3$ and ND_3 isotopomers. Prominent features of the infrared spectrum of NH_2–HF are a strongly red-shifted HF stretching mode ($\Delta\nu \approx -720$ cm^{-1} relative to that for isolated HF) and strong absorptions at 791 and 798 cm^{-1} attributed to HF librational modes in the complex. Quantum chemistry calculations reveal that the hydrogen-bonded NH_2–HF complex has a planar C_{2v} structure and a binding energy of 51 kJ/mol. Calculated hyperfine constants and vibrational frequencies of the complex are in good agreement with those observed in the EPR and IR experiments.

PACS: 82.30.Cf

1. Introduction

The dynamics of atom-molecule reactions are important in many areas of chemistry, including atmospheric chemistry, combustion/flame suppression, and chemical lasers. Long-lived intermediate complexes play a special role in such reactions because they can allow extensive energy redistribution and randomize the final scattering angles of the products. It is therefore essential to gain a detailed knowledge of reaction intermediates, especially in the region of a transition state, in order to develop a comprehensive description of any elementary chemical reaction. This type of investigation constitutes one of the most active fields of modern chemical research. Various time-resolved techniques are being used to access this part of potential energy surface of elementary gas phase reactions (see, for example, Refs. 1–3). However, low temperature spectroscopy of matrix-isolated species continues to play a prominent role due to its universality and reliability in the interpretation of experimental data. For the last 20 years, a variety of methods have been developed for stabilizing intermediates in cryogenic inert matrixes, such as freezing of reaction products from the gas discharge, photolysis and radiolysis of complexes, and laser ablation (see, for example Refs. 4–6).

Recently we have used a combination of FTIR and EPR techniques in rare gas matrices to study free radicals and radical–molecule complexes formed by reaction of fluorine atoms with small polyatomic molecules. This methodology takes advantage of the widely used matrix isolation technique for immobilizing molecular species as well as the high mobility of fluorine atoms in rare gas solids, as observed by Apkarian et al. [7,8]. The quantum yield for photodissociation of F_2 in solid argon is nearly unity if the initial kinetic energy of photogenerated «hot» F atoms is more then 0.5 eV. The «hot» F atoms formed by UV photolysis are believed to migrate over the distances approaching 3 nm [9–11]. Once thermalized, the F atoms are essentially immobile in the matrix at temperatures less than 18 K. However, at 20–26 K, F atoms are able to diffuse approximately 10 nm in a time scale 10^2–10^4 s because the barrier to thermal diffusion in

solid argon is only 4.5–5.8 kJ/mol [8]. The ability to control the mobility of F atoms through changes in temperature provides a unique opportunity to carry out solid-state chemical reaction of F atoms with isolated molecules in argon matrix. Because the crystalline environment prevents reaction products from flying apart and promotes fast relaxation of excess energy released in reaction, the stabilization and spectroscopic observation of open-shell intermediate species that are not observable in gas phase studies can be realized.

Based on these unique peculiarities of F atoms, we have determined the spectral characteristics of open-shell intermediates formed in reactions of mobile F atoms with ethene [12], methane [13,14], hydrogen [15], carbon monoxide [10,16], oxygen [16], nitric oxide [17], and ozone [18]. We have shown that the combination of two complementary spectroscopic techniques, EPR and FTIR, allows one to obtain:

a) direct evidence of a radical intermediate (by EPR spectroscopy);

b) the complete set of hyperfine (hf) constants of stabilized intermediates [14,17];

c) reliable assignments of the infrared bands of the intermediate from comparison of kinetics of radical formation obtained in EPR measurement with kinetics of growth of new bands in FTIR measurements [12,17];

d) branching ratios for reaction channels that yield closed-shell and radical products [12,16];

e) molecular structure of intermediate species in the lattice from comparisons of measured and calculated hf constants and vibration frequencies [15,16].

Particular attention has been given to H-atom abstraction reactions:

$$F + RH \rightarrow HF + R \ . \qquad (1)$$

We have observed the open-shell complexes CH_3–HF and H–HF as intermediate products in reactions of diffusing F atoms with CH_4 and H_2 molecules trapped in a matrix [13–15]. EPR spectroscopy is especially useful in these studies because the hf interaction of the unpaired electron with magnetic nuclei in the complex is very sensitive to the distance between the radical R and the HF molecule and to their mutual orientation.

In the present study, we have used this approach to study the reaction of F atoms with NH_3 molecules isolated in an argon matrix. Usually, gas phase reactions of type (1) give rise to extensive HF internal excitation and population inversions [19] which are required for laser action. However, attempts to obtain an inverted HF state distribution in

$$F + NH_3 \rightarrow HF + NH_2 \ , \quad \Delta H_0 \approx -130 \text{ kJ/mol} \qquad (2)$$

were unsuccessful, despite its high exothermicity [20,21]. It was assumed that the failure was due to formation of a long-lived FNH_3 species during the reaction. The existence of such an intermediate complex causes randomization of the exoergicity among its internal modes. *Ab initio* calculations performed by Goddard et al. [22] predicted that the NH_2–HF formed in the exit channel of reaction (2) should be bound by ~ 50 kJ/mol (~ 33 kJ/mol when corrected for zero-point energy effects). In our preliminary EPR study [23,24], we observed the intermediate complex NH_2–HF for the first time. In this paper, we report a detailed EPR, FTIR and computational study of this reaction intermediate to obtain the total set the hf constants and vibrational frequencies. The results show that the structure of the complex and binding energy is close to predictions of Goddard et al. [22], and that the complex suffers only a minor distortion in the argon lattice relative to its gas phase equilibrium geometry.

2. Experimental

The experimental technique used was described in detail elsewhere [14]. Briefly, solid argon films doped with reactant molecules were formed by vapor deposition of Ar–NH_3 and Ar–F_2 gas mixtures through separate inlets onto a substrate at 15 K (sapphire for EPR experiments; CsI for the infrared study). The sample composition was typically Ar:NH_3:F_2 = 1000:1:1. Infrared spectra were recorded with a Mattson Model RS/1000 FTIR spectrometer (spectral region from 500 to 4000 cm^{-1} and spectral resolution 0.5 cm^{-1}).

In the EPR experiments (performed in Russia), argon (99.9995%) and fluorine (99.9%) were used without purification. Ammonia $^{14}NH_3$ (and $^{15}NH_3$) was used after drying over NaOH. Deuterated ammonia, ND_3 , was prepared by repeated exchange of NH_3 with D_2O followed by distillation and drying over NaOD. The deuterium isotopic purity was estimated at 90%. In FTIR experiments (performed in the United States), argon (Spectra gases, 99.999%), fluorine (Spectra gases, 10% in argon), NH_3 (Matheson) and ND_3 (Cambridge Isotope Laboratories Inc., D, 99%) were used without further purification.

Fluorine atoms were generated by UV photolysis of F_2 molecules using 337 nm laser light in the EPR experiments, and 355 nm laser light in the infrared experiments. The average laser power did not exceed 20 mW/cm^2 in either type of experiment. To distinguish the chemical reactions involving photogenerated «hot» F atoms from those of diffusing thermal atoms, photolysis of F_2 molecules was performed at 15 K and the samples were subsequently annealed in a separate step.

EPR spectra of freshly prepared samples exhibit no lines due to paramagnetic species. Very weak infrared bands of CO_2 (661.9 and 2340.5 cm^{-1}) were found in the IR spectra of deposited samples. A sharp absorption assigned to FO_2 (1490 cm^{-1}) appears in the spectra of photolyzed samples at 20–25 K. Oxygen is a common impurity in fluorine gas and is difficult to remove by fractional distillation.

3. Results and discussion

3.1. EPR spectra of dilute mixtures Ar:NH_3:F_2 = *1000:1:1 photolyzed at 15 K.* A complex anisotropic spectrum consisting of two series of lines (shown in Fig. 1,*a*) is produced by 337 nm laser photolysis at 15 K. In the initial stage, the intensity of the EPR lines is proportional to the photolysis period, but approaches a limiting value under exhaustive photolysis due to depletion of the F_2 concentration. Temperature-induced changes of line shapes and intensities are reversible in the range 7.7–18 K, which shows that the concentration of radicals does not change after completion of photolysis. Lowering the temperature causes a broadening of most of the anisotropic lines, whereas lines in the other series are narrowed. Only 9 narrow lines remain in the spectrum at 7.7 K, as shown in Fig. 1,*b*. Thus, the spectra correspond to the superposition of spectra of at least two products. The EPR spectrum of the radical whose lines are narrowed upon cooling consists of 9 lines: a 1:1:1 triplet of triplets with hf splittings of 1.05 and 2.40 mT, and $g = 2.0058$. Recall that only absolute values of hf constants are determined in EPR experiments usually. The hf constants and g-factor are all in good agreement with the data of Cochran et al. [25] obtained for the radical NH_2 in solid argon at 4.2 K (a_H = 2.38 mT, a_N = 1.04 mT and $g = 2.0049$).

To elucidate the unusual temperature behavior of EPR lines of NH_2 radical in temperature region 7.7–15 K, a series of additional experiments was carried out. The samples Ar:NH_3 = 1000:1 were irradiated by a deuterium lamp at 7.7 K to generate stabilized NH_2 radicals. EPR spectra of NH_2 radical at different temperatures are shown in Fig. 2. The spectrum detected at 7.7 K corresponds to the spectrum of NH_2 radical shown in Fig. 1,*b*. There are three prominent features of the spectrum of stabi-

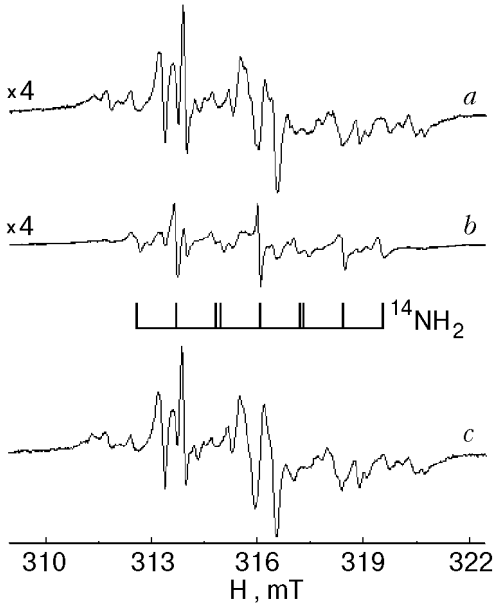

Fig. 1. EPR spectra of the Ar:NH_3:F_2 = 1000:1:1 sample after exhaustive photolysis at 15 K (*a*); after subsequent cooling to 7.7 K (*b*); after annealing of the photolyzed sample for 30 min at 25 K and subsequent lowering the temperature to 15 K (*c*). Intensities of the spectra are corrected in accordance with the Curie law.

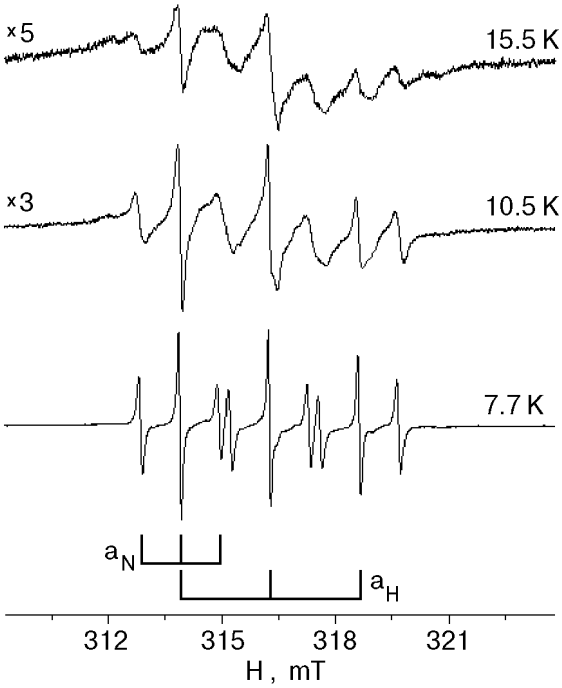

Fig. 2. EPR spectra of NH_2 radical generated by UV photolysis of NH_3 molecules in solid argon at different temperatures.

lized NH_2 . The first and well-known peculiarity is that two equivalent hydrogens of NH_2 yield triplet pattern 1:1:1, instead of the expected 1:2:1 at 7.7 K [25]. The second is that different line widths are observed for components corresponding to different nuclear projections of the N atom. The third feature of this spectrum is the unusual temperature broadening of the EPR lines observed in this study.

Because the same spectral lines of NH_2 in Ar:NH_3 mixtures are observed following photolysis of Ar:NH_3:F_2 samples, we may conclude that NH_2 is one of the photolysis products formed in reaction (2) of photogenerated «hot» F atom with NH_3 molecule. However, the NH_2 concentration did not exceed 15% of the total concentration of radicals.

3.2. EPR spectra of products forming upon annealing of the samples Ar:NH_3:F_2 *photolyzed at 15 K.* To initiate reaction of diffusing thermal F atoms, we annealed the photolyzed samples at temperatures $T > 20$ K. The post-annealing EPR spectrum (measured at 15 K) is shown in Fig. 1,*c*. Comparison of the spectra before (Fig. 1,*a*) and after annealing shows that concentration of NH_2 radicals does not change, but the intensity of lines of the other radical increase approximately fourfold due to reaction of F atoms that diffuse through the argon matrix. The EPR lines of this radical become narrow and isotropic at temperatures above 30 K, as shown in Fig. 3,*a*. The spectrum consists of narrow lines (~ 0.1 mT) formed from a 1:1:1 triplet splitting with $a_1 = 1.20$ mT, a 1:2:1 triplet

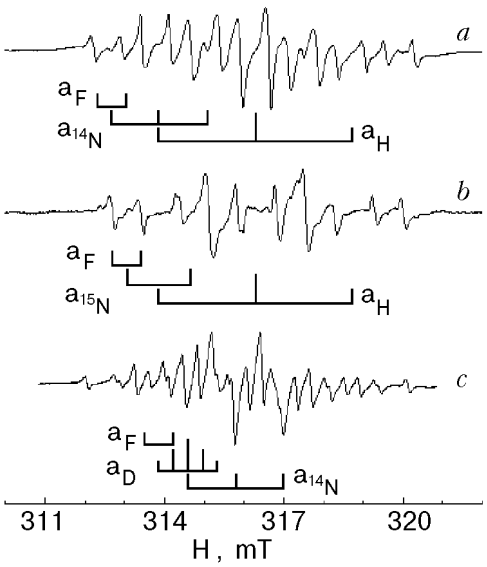

Fig. 3. EPR spectra of the samples after photolysis at 15 K and subsequent annealing at 25 K: Ar:$^{14}NH_3$:F_2 (*a*); Ar:$^{15}NH_3$:F_2 (*b*); Ar:$^{14}ND_3$:F_2 (*c*). All spectra were recorded at 35 K. (The $^{14}ND_3$ used in experiments contains ~ 10% $^{14}NH_3$; therefore, the weak outer lines in this spectrum correspond to $^{14}NH_2$–HF).

with $a_2 = 2.40$ mT, and a doublet $a_3 = 0.70$ mT. Because $a_2 \approx 2 \times a_1$, four of the lines are unresolved due to accidental overlapping. Thus, only 14 lines are observed in the spectrum, instead of the usual 18 lines associated with a triplet of triplets of doublets. Two of the triplet splittings, a_1 and a_2 , are similar to those of the NH_2 radical, and this allows us to ascribe the doublet splitting a_3 to the magnetic interaction with one of the magnetic nuclei of the HF molecule bound to the complex NH_2–HF. In order to distinguish the hf constants on H, F and N nuclei, we have performed a series of similar experiments with isotopically substituted ammonia.

EPR spectra obtained after photolysis and annealing of matrices containing Ar:$^{15}NH_3$:F_2 and Ar:ND_3:F_2 are shown in Figs. 3,*b* and 3,*c*, respectively. Referring to Fig. 3,*b*, the use of $^{15}NH_3$ leads to replacement of the triplet ($a_N(^{14}N) = 1.20$ mT) by a doublet ($a_N(^{15}N) = 1.55$ mT), while two other splittings, a_2 and a_3 , remain the same. In the samples containing ND_3 , the triplet ($a_H = = 2.40$ mT) is replaced by a quintet ($a_D = 0.37$ mT). These results permit a definitive assignment of the hf constants a_1 and a_2 to the NH_2 group. The last doublet splitting a_3 (which was unchanged by isotopic substitution) is ascribed to the ^{19}F atom, because it is only other atom in the system having a nuclear spin $I = 1/2$. Because NH_2F is a closed-shell molecule, we can attribute the EPR spectrum to the radical-molecule complex NH_2–HF, presuming that the hf constant of the H atom of the HF molecule a_H is less than spectral resolution 0.05 mT.

Therefore, the main product in the reactions of photogenerated «hot» and thermally diffusing F atoms with isolated ammonia is the open-shell complex NH_2–HF:

$$F + NH_3 \longrightarrow NH_2\text{–}HF\ . \qquad (3)$$

3.3. Infrared absorption spectra of dilute mixtures Ar:NH_3:F_2 = *1000:1:1 photolyzed at 15 K.* The NH_3 molecules trapped in rare gas matrices at low temperatures have been the subject of numerous experimental studies [26-28]. It was shown that the ν_2 bending vibrational mode for NH_3 in argon matrix exhibits several well-resolved bands, which can be assigned to transitions involving rotation and inversion of the NH_3 molecule. Assignment of these bands, given by Abouaf-Margulin et al. [27], is shown in Fig. 4,*a* for the sample Ar:NH_3:F_2 = 1000:1:1. The band at 1000 cm^{-1}, labeled *A* in Fig. 4,*a*, is due to dimers of NH_3 [27]. The broad band at 966 cm^{-1}, labeled *K* in Fig. 4,*a*,

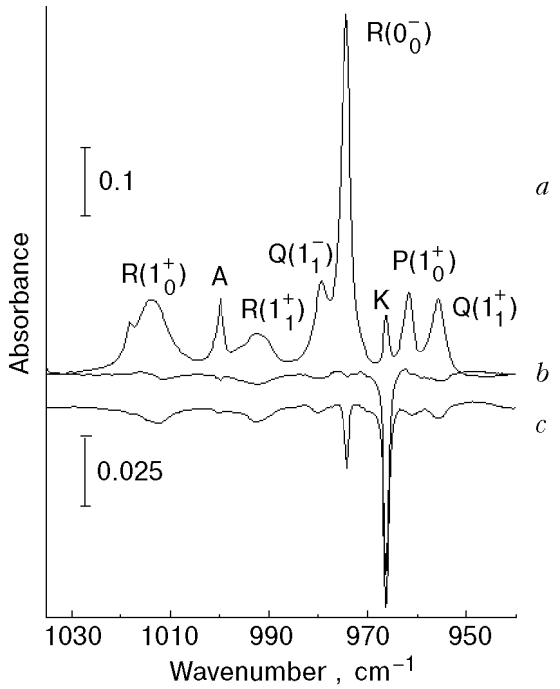

Fig. 4. Infrared spectra of the ν_2 region of NH_3 in Ar:NH_3:F_2 = 1000:1:1 sample at 15 K (trace *a*). Traces *b* and *c* are difference spectra showing changes of band intensities after 20 min and 300 min photolysis 355 nm at power 10 mW/cm^2, respectively.

was assigned earlier by Andrews and Lascola [29] to the reactant complex [F_2–NH_3]. These authors ascribed a new weak absorption at 781 cm^{-1} to the perturbed F_2 vibrational mode in this complex. Our experimental evidence supports their assignment of these bands: both of them (966 and 781 cm^{-1}) appear in samples containing F_2 and NH_3 molecules only, and their intensities are proportional to the concentration of F_2 molecules in Ar:NH_3:F_2 samples.

The kinetics of UV photolysis of the Ar:NH_3:F_2 samples exhibit two characteristic times. Infrared bands of the complex [F_2–NH_3] are totally destroyed in the initial stage of photolysis: $\tau_1 \approx 10$ min for a photolysis laser intensity of 10 mW/cm^2. Prolonged photolysis leads to a reduction of IR bands of isolated NH_3 molecules as shown in Figs. 4,*b* and 4,*c*. Only about 1–2% of the NH_3 is consumed after exhaustive photolysis, and the time scale for this process is $\tau_2 \approx 200$ min under the same conditions as above.

Photolysis reveals two new series of bands. The first series grows in the initial stage at the same rate as the disappearance of the [F_2–NH_3] complexes. These product bands were observed by Andrews and Lascola previously [29] and were attributed to the closed-shell product complex NH_2F–HF:

$$[F_2\text{–}NH_3] \xrightarrow{h\nu} NH_2F\text{–}HF \ . \qquad (4)$$

The second series of new bands appears at 3267, 1512, 1465, and 797 (791) cm^{-1} under prolonged photolysis ($\tau_2 \approx 200$ min). Also, weak sharp absorptions in the 3800–3900 cm^{-1} region appear due to formation of isolated HF molecules [30]. Their intensities are 10–20 times less intense than the band at 3267 cm^{-1}. Growth of this second series of bands occurs at the same rate as consumption of isolated NH_3 .

Using the difference in photochemical reaction rates, we can distinguish photoinitiated reactions in complexes from reactions of translationally «hot» F atoms formed from photolysis of isolated F_2 molecules. The photodissociation quantum yield of F_2 in solid argon at 355 nm is $\Phi_0 \approx 0.3$–0.5 [7]. The photodissociation rate $k_d = \sigma I \Phi_0$ (where $\sigma = 10^{-20}$ cm^2 is absorption cross-section F_2 , and I is light intensity) is very close to the observed «slow» photochemical reaction rate $(\tau_2)^{-1}$. Therefore, we may conclude that consumption of isolated NH_3 and corresponding formation of new products (the second series of bands plus HF) result from the reaction of translationally «hot» F atoms with isolated NH_3 molecules.

3.4. Annealing of the samples Ar:NH_3:F_2 *photolyzed at 15 K.* Annealing of photolyzed samples was carried out by step-by-step procedure. After completion of photolysis at 15 K, the sample was annealed for 3–5 min at 25 K. Then the temperature was lowered back to 15 K, and the IR spectrum was recorded. This cycle of photolysis (annealing)

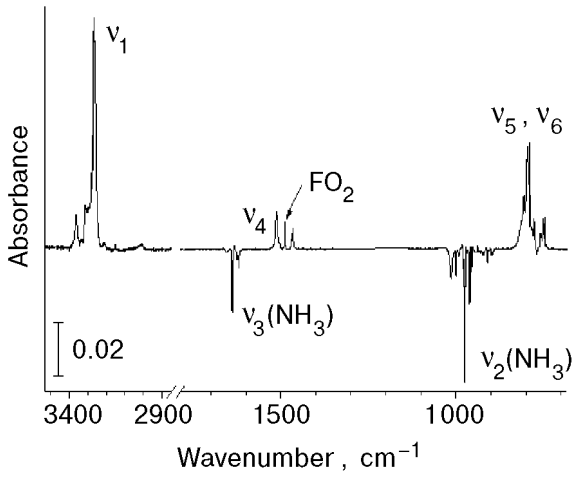

Fig. 5. Difference spectrum of photolyzed sample Ar:NH_3:F_2 = 1000:1:1 before and after annealing at 25 K. Spectra were recorded at 15 K.

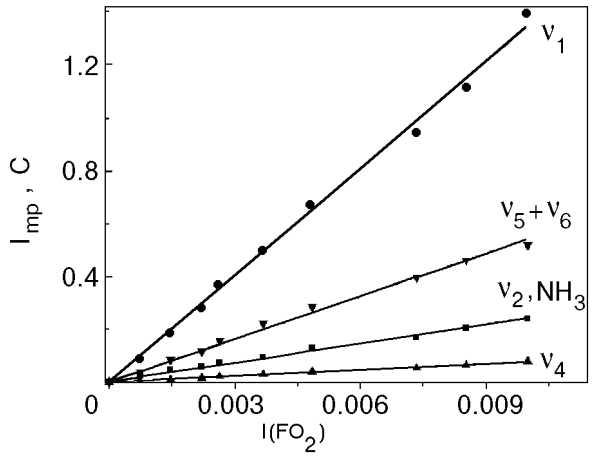

Fig. 6. Growth of the intensities I_{mp} of the major product bands and consumption C of the NH_3 band vs. intensity I of the FO_2 (1490 cm^{-1}) band during annealing of the photolyzed sample Ar:NH_3:F_2 .

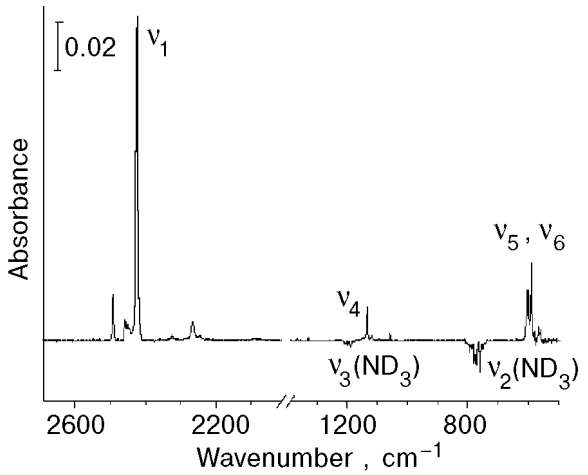

Fig. 7. Difference spectrum of a photolyzed sample Ar:ND_3:F_2 = 1000:1:1 before and after annealing at 25 K. Spectra were recorded at 15 K.

spectrum was repeated 10–12 times until reaction was complete. The final IR spectrum is shown in Fig. 5. Annealing is accompanied by consumption of isolated NH_3 molecules and the growth of the same series of intense bands at 3267, 1512, 1465, and 797(791) cm^{-1} that appeared upon prolonged photolysis. In addition, a sharp band at 1490 cm^{-1} due to FO_2 radical appeared also. This radical is formed by addition reaction of diffusing F atoms with impurity O_2 molecules, as was shown in our previous study [16]:

$$F + O_2 \longrightarrow FO_2 . \qquad (5)$$

Although the presence of a minor O_2 impurity might be viewed as a nuisance, we have used reaction (5) as an internal standard for characterizing the reaction rate of diffusing F atoms during the annealing cycles. Figure 6 shows the intensities of the major product bands and decrease of NH_3 band relative to the FO_2 band upon annealing of the sample. The linear dependences of changes in the band intensities provide convincing evidence that

Table 1

Vibrational frequencies of the complex NH_2–HF (ND_2–DF)

Assignment	Wavenumber, cm^{-1}			
	NH_2–HF		ND_2–DF	
	expt.	calc.[a)]	expt.	calc.
$\nu_1(a_1)$ HF str.	3267 (17.5)	3486	2423 (17.5)	2531
$\nu_2(b_2)$ NH_2 str. asym	3211 tentatively	3497 (0.4)		2575 (0.5)
$\nu_3(a_1)$ NH str. sym		3401 (0.4)		2458 (0.1)
$\nu_4(a_1)$ NH_2 bend	1512 (1.0)	1527 (1.0)	1132 (1.0)	1127 (1.0)
$2\nu_5$ or $2\nu_6$	1465 (0.4)		1056 (0.05)	
$\nu_5(b_2)$ HF libration (in-plane)	797 (3.1)	860 (6.3)	601 (3.2)	622 (4.5)
$\nu_6(b_1)$ HF libration (out-of plane)	791 (3.4)	817 (8.5)	587 (3.5)	596 (6.8)
$\nu_7(b_1)$		280		212
$\nu_8(a_1)$ hydrogen-bond stretch		257		244
$\nu_9(b_2)$		221		164

[a)] Relative integrated intensities of bands are given in parentheses

this series corresponds to a primary reaction product of diffusing thermal F atoms with isolated NH_3 molecules. Note that the reaction of thermal F atoms consumes ~ 10% of NH_3 molecules, about 5 times greater than the yield during exhaustive UV photolysis at 15 K.

As we have concluded in the EPR study, the main reaction product of photogenerated «hot» and thermal F atoms with isolated ammonia is the open-shell complex, NH_2–HF. To assign the observed IR bands, we have performed similar experiments with ND_3 .

The infrared spectrum of a photolyzed and annealing sample Ar:ND_3:F_2 is shown in Fig. 7. It illustrates the consumption of isolated ND_3 molecules (series of bands in the ν_2 and ν_3 regions of ND_3 at 760 and 1200 cm^{-1}) and the growth of a series of new bands at 2423, 1132, 1056, and 601(587) cm^{-1}. Growth of these products bands and diminution of ND_3 bands are linear with increasing intensity of the FO_2 band at 1490 cm^{-1}, similar to the result with NH_3 . It is apparent that the number of new product bands and their pattern of intensities correlate closely with the NH_3 results, as shown in Table 1. This permits a straightforward determination of the isotopic shifts. For example, the isotopic shift for the strongest band at 3267 cm^{-1}, $\Delta\nu = 844$ cm^{-1}, is close to that calculated for a pure HF vibration $\Delta\nu = 898$ cm^{-1}. Since the infrared band of HF molecule isolated in argon lies at $\nu > 3900$ cm^{-1}, the position of its absorption below 3700 cm^{-1} is characteristic of an HF molecule that is strongly hydrogen-bonded with another molecule [31]. Thus, we definitively assign this band to HF molecule in the complex. The band at 1512 cm^{-1} lies very close to the ν_2 bending vibration of NH_2 in solid argon, 1523 cm^{-1} [32]. Its observed isotopic shift $\Delta\nu = 385$ cm^{-1} is in good agreement with calculated $\Delta\nu = 440$ cm^{-1}, hence, we attribute this band to the ν_2 bending of the NH_2 group of the NH_2–HF complex.

The combined results of the EPR and infrared experiments provides clear and convincing evidence that the primary reaction product of F atoms with isolated NH_3 molecules in solid argon is the open-shell complex, NH_2–HF. A detailed description of the infrared bands is given below, based on the observed data and vibrational analysis for calculated structure of the NH_2–HF complex.

3.6. Calculated structure and vibrational analysis of the NH_2–HF *complex*. We carried out quantum chemical calculations in order to clarify the structure of the NH_2–HF complex, and to establish its spectroscopic characteristics (hyperfine constants and fundamental vibrations). All of computations were performed using Gaussian 98 suite of codes [33]. A density functional method B3LYP with AUG-cc-pVTZ basis set was used for geometry optimization and calculation of the spectroscopic characteristics.

The NH_2–HF complex has a planar equilibrium structure with C_{2v} symmetry. The optimized geometry is similar to that calculated earlier by Goddard et al. [22]. The binding energy of the complex is equal to 51 kJ/mol (34 kJ/mol when corrected for zero-point energy effects). The geometry and both experimental and calculated isotropic hf constants of the complex are given in the scheme

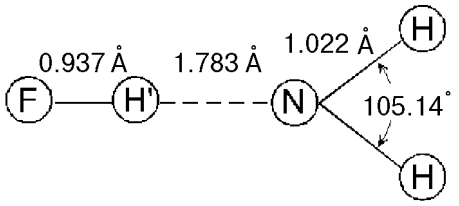

a(calc), mT	–0.70	0.02	1.15	–2.30
a(exp), mT	0.70	<0.05	1.20	2.40

(6)

Calculated hf constants a_N , a_H , and a_F are in good agreement with those obtained in experiment. The calculated hf constant at the proton of the HF molecule a_H is less than 0.05 mT and, as was noted above, could not be resolved under our experimental conditions.

The calculated frequencies and relative intensities of IR bands for NH_2–HF and ND_2–DF complexes are listed in Table 1. If the HF molecule is bound to the radical-molecule complex, its two rotational degrees of freedom become two HF librational modes in the complex (ν_5 , ν_6), whereas the HF fundamental (ν_1) remains in the complex. These fundamentals give rise to very strong infrared absorptions that are predicted by the calculations and observed in the experiments for both NH_3 and ND_3 isotopomers. The three translational degrees of freedom become a hydrogen-bond stretching mode (ν_8) and two bending modes of the complex (ν_7 , ν_9); these fundamentals occur at low frequencies and give rise to much weaker absorptions.

A relatively weak band at 1465 cm^{-1} of NH_2–HF could be ascribed to one of overtones $2\nu_5$, or $2\nu_6$, or possibly both of them because a shape of this band shows superimposition of two unresolved bands split by 2–3 cm^{-1}. In the deuterated complex, this band lies at 1056 cm^{-1}, and its relative

intensity is about 10 times less than for the normal proteated complex, providing support for the assignment as an overtone.

In general, the agreement with the calculated and observed frequencies and isotopic shifts is excellent. The single exception is a ~ 200 cm^{-1} difference between the observed and calculated frequency of the HF stretch vibration in the complex. This is likely due to anharmonicity of the intramolecular and intermolecular potentials [34,35]. The calculations predict weak intensities for the NH stretching vibrational modes of the complex. In the IR spectrum, a weak broad band at 3007 cm^{-1} in Ar:NH_3:F_2 (2265 cm^{-1} in Ar:ND_3:F_2) is observed (see Figs. 5 and 7). We tentatively assign this band to the NH asymmetric stretch, although a reasonable alternative assignment could be to the HF stretch in the complex located in a perturbed lattice site.

In our previous paper we calculated the charge distribution in the complex NH_2–HF [24]. In line with this distribution, we have concluded that the contribution of electrostatic intermolecular interaction to the binding energy of the complex is 12–15 kJ/mol, i.e., ~ 25% of the total binding energy. On this basis, we conclude that the NH_2–HF complex has significant covalent bonding character, and the nature of the intermolecular bond should be similar to that in the hydrogen-bonded NH_3–HF complex [36]. It was shown earlier that displacement of fundamentals of a hydrogen-bonded complex below their isolated value and the appearance strong infrared absorptions originated from librational modes in the complex are indicative of a strong intermolecular hydrogen bond [37]. Although various hydrogen-bonded molecular complexes M–HF were studied by spectroscopic methods [38,39], to our knowledge there are no systematic data on thermodynamics of the hydrogen-bonded molecular complexes M–HF. Thus we can compare our data with those for well-studied strong hydrogen-bonded complex NH_3–HF only. The energy of hydrogen bond, 64 kJ/mol, was calculated by several quantum chemistry methods [36]. Infrared absorptions of this complex were detected at 3041(ν_1) and 916 cm^{-1} (2-fold degenerate ν_5) in an argon matrix by Andrews [31]. Comparison of these bands with those obtained for NH_2–HF shows that the binding energy of the NH_2–HF complex should be comparable to that of NH_3–HF. Hence the calculated binding energy of NH_2–HF complex, 51 kJ/mol, is quite reasonable.

3.7. Arrangement NH_2–HF *complex in an argon lattice*. Starting from the calculated structure we performed a geometry optimization of the NH_2–HF complex in an argon lattice. A detailed description of energy minimization procedure for NH_2–HF located in a substitutional site of an argon cluster containing 365 atoms was given earlier in previous paper [23,24]. In the first step, we have used the «hard» collinear complex obtained in computations (scheme 6). In those calculations, the complex retained its collinear structure and sizes. The resulting arrangement of the complex in Ar cluster is shown in Fig. 8. The position of the nitrogen atom of the NH_2 group is close to the center of the substitutional site (0,0,0). At the other end of the complex, the fluorine atom of the HF molecule occupies the nearest octahedral interstitial site O_h ($-a/2$,0,0), where a = 0.54 nm is the parameter of Ar lattice. Obviously, any external forces directed along the C_2 axis of the complex should induce an out-of-plane deformation and should lower the symmetry of the complex from C_{2v} to C_s. To investigate this possibility, we performed additional calculations that included two floppy coordinates of the complex: the distance between N and H′ atoms, $R_{NH'}$, and the out-of-plane angle α:

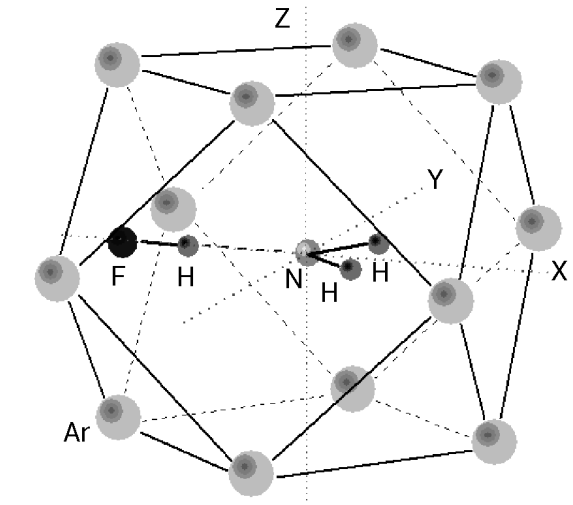

Fig. 8. Arrangement of the complex NH_2–HF in argon lattice. Twelve nearest-neighbor argon atoms are shown.

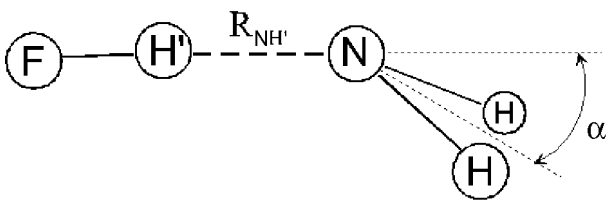

(7)

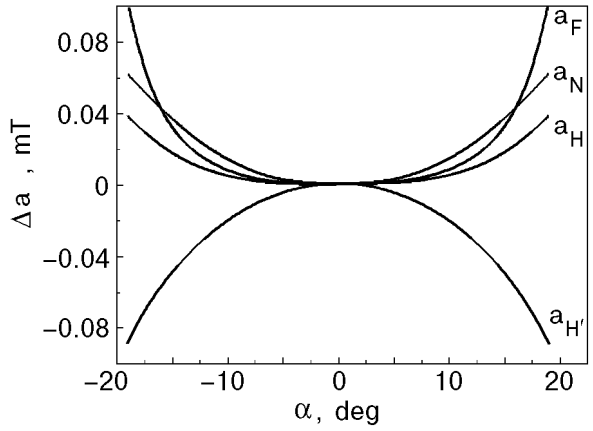

Fig. 9. Differences between the calculated isotropic hyperfine constants of NH_2–HF and those for the equilibrium geometry as a function of the out-of-plane bending angle α.

The corresponding force constants $k_R = 24$ N/m and $k_\alpha = 5.3$ N/m were obtained from quantum chemistry calculations. Optimization of this «floppy» complex in the lattice results in a slight distortion of its geometry: $\Delta R_{NH'} = 0.001$ nm, and $\alpha \le 4°$. Such minor deformations of the complex are probably due to the near coincidence between the N–F distance and one-half the lattice period, $a/2$. The good fit of this molecule extends to the perpendicular axes as well, as shown in Fig. 8. The two nearest argon atoms along the x-axis, located at $(a,0,0)$ and $(-a,0,0)$, shift only +0.002 and −0.0016 nm from their initial (undistorted) positions, respectively.

The calculated hf constants are sensitive to the out-of-plane bending angle α, particularly if α is greater than 10° (Fig. 9). Based on the excellent agreement of the measured hf constants with those calculated for the C_{2v} structure, we may conclude that the complex suffers at most a minor distortion in the argon lattice relative to its gas phase equilibrium geometry. This conclusion is further supported by the fact that the observed HF librational modes in the complex ν_5 and ν_6 are nearly degenerate, like the doubly degenerate bending mode in a linear triatomic molecule.

3.8. Rotation of NH_2 *in an argon lattice.* As shown in the previous sections, two types of radical products are observed: NH_2–HF complexes and isolated NH_2 free radicals. The EPR spectrum of the complex is anisotropic at 15 K, and thermal averaging of the anisotropic magnetic interactions in the complex occurs only at temperatures above 30 K, as shown in Fig. 3. Because the complex has a large size along its C_2 axis, it is difficult to imagine that the averaging of the anisotropic interactions occurs by reorientation of this axis in the lattice. Our calculations show that the barrier to this type of rearrangement is high, ~ 4–12 kJ/mol. It is more likely that the averaging of anisotropy occurs via intramolecular bending vibrations in the complex and large amplitude libration of the NH_2 group in the lattice.

Figures 1 and 2 illustrate that the EPR spectrum of the isolated NH_2 radical exhibits the aforementioned unusual 1:1:1 triplet splitting of the protons. In contrast, the expected 1:2:1 triplet splitting for two equivalent protons of NH_2 group is observed in the EPR spectrum of the NH_2–HF complex. McConnel [40] attributed the 1:1:1 triplet pattern of NH_2 to free rotation in the argon lattice at 4.2 K. The Pauli principle requires that the overall symmetry of the wave function is antisymmetric with respect to permutation of the two protons. The electronic wave function is antisymmetric with respect to rotation about the C_2 axis. Therefore, rotational states having even J quantum numbers (0, 2, 4, etc.) are uniquely associated with the symmetric proton nuclear spin state ($I_H = 1$). Conversely, odd-J states are associated with the antisymmetric $I_H = 0$ proton nuclear spin state. Given the small rotational moment for rotation about the C_2 axis, most of the NH_2 radicals are in the $J = 0$ rotational level at argon matrix temperatures, and we should expect to observe the three components of the EPR hyperfine structure with equal intensities.

However, Jen [41] pointed out that this mechanism cannot explain the different line widths of components of the EPR spectrum having different nuclear projections of the N atom. This means that the anisotropy of magnetic interactions is not completely averaged due to hindered (noncoherent)

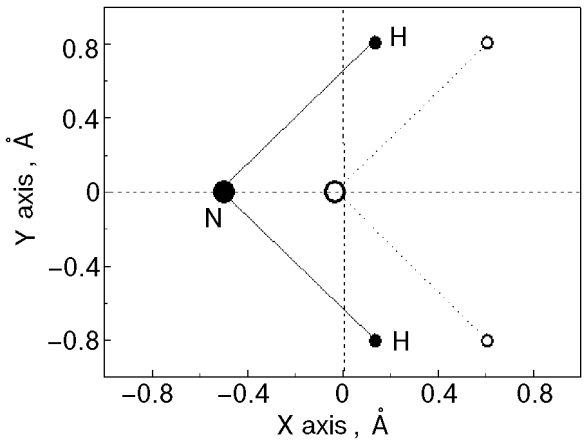

Fig. 10. Arrangement of the NH_2 radical in an argon lattice. Direction of axes coincides with those of the lattice shown in Fig. 8.

rotation. The apparent contradiction can be resolved if the stabilized NH_2 has one rotational degree of freedom around C_2 axis only, whereas rotations around of another axes of radical are strongly hindered in a lattice. Figure 10 shows calculated arrangement of NH_2 radical in substitution site of argon lattice. The NH_2–HF complex, in contrast, exhibits a normal 1:2:1 hyperfine splitting due to the proton nuclear spins. The important distinction is that whereas rotation about the C_2 axis is essentially unrestricted for NH_2 (calculated barrier of E_b = 420 J/mol), the corresponding motion in the NH_2–HF complex is strongly hindered (calculated barrier E_b = 2100 J/mol). Perturbation of rotational motion in the solid phase was first studied by Pauling [42] and Devonshire [43], who calculated energy levels for a linear molecule in a field with O_h symmetry. They showed that the lowest energy level of a strongly hindered rotor is a doublet that has both symmetric and antisymmetric components, as shown in Scheme 8:

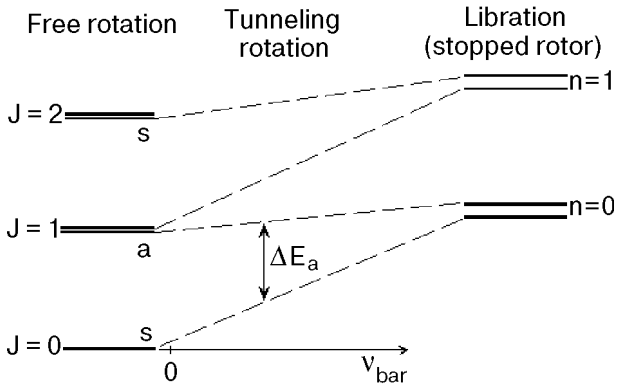

(8)

In this case, both proton nuclear spin states are represented equally, resulting in the familiar 1:2:1 hyperfine splitting pattern in the EPR spectrum.

4. Conclusions

In the present research we have demonstrated that the combined use of infrared and EPR spectroscopic techniques to study radical intermediates formed in solid-state chemical reaction of mobile F atoms enabled us to observe and make reliable assignments for the hyperfine constants and vibrational frequencies. It was shown that the geometry of the stabilized intermediate can be determined by comparison of the measured spectroscopic data with those from quantum chemistry calculations. The main results of this study are the next.

1. The radical-molecule complex NH_2–HF is observed as an intermediate product in the reactions of mobile F atoms with NH_3 molecules trapped in solid argon.

2. The EPR spectrum of NH_2–HF is characterized by three hyperfine splittings: the 1:1:1 triplet with a_N = 1.20 mT, the 1:2:1 triplet with a_H = 2.40 mT, and the doublet splitting a_F = = 0.7 mT. The hf constant at H atom of HF molecule is less than 0.05 mT.

3. A strong red shift of the HF band relative to isolated HF, $\Delta\nu \approx 720$ cm^{-1}, is observed in the infrared spectrum of NH_2–HF complex. The next prominent feature is a strong doublet band at ~ 800 cm^{-1} that corresponds to the two in-plane and out-of-plane HF librational modes of the complex, ν_5 and ν_6 . These features of IR spectrum of the complex are indicative of the relatively strong intermolecular hydrogen bond in the complex.

4. Density functional calculations revealed that the NH_2–HF complex has a planar C_{2v} structure and a binding energy of 51 kJ/mol (34 kJ/mol when corrected for zero-point energy effects). Calculated hf constants of the complex are in good agreement with those observed in EPR experiment. Calculated vibrational frequencies for NH_2 bending and HF librational modes in the complex ν_5 and ν_6 correspond well to those obtained in FTIR measurements. The ~ 200 cm^{-1} difference between the observed and calculated frequency of the HF stretching vibration in the complex is due to anharmonicity of the intramolecular and intermolecular potentials.

5. If the C_2 axis of the NH_2–HF complex coincides with the C_4 axis of the host fcc argon crystal, then the interaction with lattice atoms induces only minor distortions to the equilibrium structure relative to that in the gas phase. However, the interactions between the complex and host argon atoms hinder rotation of the NH_2 group about its C_2 axis, whereas this motion is essentially unrestricted in isolated NH_2 .

Acknowledgments

We thank the Russian Foundation for Basic Research (Grant 98-03-33175) and the U.S. National Science Foundation (Grant CHE-9970032) for supporting this research.

1. Y. T. Lee, *Ber. Bunsen Ges. Phys. Chem.* **74**, 135 (1974).
2. A. H. Zewail, *Science* **242**, 1645 (1988).
3. K. Liu, J. C. Polany, and S. Yang, *J. Chem. Phys.* **98**, 5431 (1993).
4. M. E. Jacox, in: *Chemistry and Physics of Matrix Isolated Species*, Elsevier (1989).

5. L. Andrews, *J. Phys. Chem.* **88**, 2940 (1984).
6. L. B. Knight, Jr., in: *Chemistry and Physics of Matrix Isolated Species*, Elsevier (1989).
7. H. Kunntu, J. Feld, R. Alimi, A. Becker, and V. A. Apkarian, *J. Chem. Phys.* **92**, 4856 (1990).
8. J. Feld, H. Kunntu, and V. A. Apkarian, *J. Chem. Phys.* **93**, 1009 (1990).
9. R. Alimi, R. B. Gerber, and V.A. Apkarian, *J. Chem. Phys.* **92**, 3551 (1990).
10. E. Ya. Misochko, A. V. Akimov, and C. A. Wight, *Chem. Phys. Lett.* **293**, 547 (1998).
11. V. A. Apkarian and N. Schwentner, *Chem. Rev.* **99**, 1481 (1999).
12. E. Ya. Misochko, A. V. Benderskii, and C. A. Wight, *J. Phys. Chem.* **100**, 4496 (1996).
13. E. Ya. Misochko, A. V. Benderskii, A. U. Goldschleger, V. A. Akimov, and A.F. Shestakov, *J. Am. Chem. Soc.* **117**, 11997 (1995).
14. E. Ya. Misochko, A. V. Benderskii, A. U. Goldschleger, V. A. Akimov, A. V. Benderskii, and C. A. Wight, *J. Chem. Phys.* **106**, 3146 (1997).
15. A. U. Goldschleger, E. Ya. Misochko, V. A. Akimov, I. U. Goldschleger, and V. A. Benderskii, *Chem. Phys. Lett.* **267**, 288 (1997).
16. E. Ya. Misochko, A. V. Akimov, and C. A. Wight, *Chem. Phys. Lett.* **274**, 23 (1997).
17. E. Ya. Misochko, V. A. Akimov, I. U. Goldschleger, A. I. Boldyrev, and C. A. Wight, *J. Am. Chem. Soc.* **121**, 405 (1999).
18. E. Ya. Misochko, A. V. Akimov, and C. A. Wight, *J. Phys. Chem.* **A103**, 7972 (1999).
19. B. E. Holmes and D. W. Sester, in: *Physical Chemistry of Fast Reactions* **2**, Plenum Press, New York (1979).
20. D. J. Donaldson, J. J. Sloan, and J. D. Goddard, *J. Chem. Phys.* **82**, 4524 (1985).
21. S. Wategaonkar and D. W. Sester, *J. Chem. Phys.* **86**, 4477 (1987).
22. D. Goddard, D. J. Donaldson, and J. J. Sloan, *Chem. Phys.* **114**, 321 (1987).
23. I. U. Goldschleger, A. V. Akimov, and E. Ya. Misochko, *Mendeleev Commun.* No. 4, 132 (1999).
24. I. U. Goldschleger, A. V. Akimov, and E. Ya. Misochko, *J. Molec. Struct.* (in press).
25. E. L. Cochran, F. J. Adrian, V. A. Bowers, *J. Chem. Phys.* **51**, 2759 (1969).
26. G. C. Pimentel, M. O. Bulanin, and M. Van Thiel, *J. Chem. Phys.* **36**, 500 (1962).
27. L. Abouaf-Margulin, M. E. Jacox, and D. E. Milligan, *J. Mol. Spectros.* **67**, 34 (1977).
28. B. Guathier-Roy, P. Boissel, L. Abouaf-Margulin, J. Pourcin, and P. Verlaque, *J. Mol. Spectros.* **115**, 147 (1986).
29. L. Andrews and R. Lascola, *J. Amer. Chem. Soc.* **109**, 6243 (1987).
30. M. T. Bowers, G. I. Kerley, and W. H. Flygare, *J. Chem. Phys.* **45**, 3399 (1966).
31. L. Andrews, *J. Phys. Chem.* **88**, 2940 (1984).
32. D. E. Milligan and M. E. Jacox, *J. Chem. Phys.* **43**, 4487 (1965).
33. M. J. Frisch, G. W. Trucks, H. B. Schlegel, G. E. Scuseria, M. A. Robb, J. R. Cheeseman, V. G. Zakrzewski, J. A. Montgomery, Jr., R. E. Stratmann, J. C. Burant, S. Dapprich, J. M. Millam, A. D. Daniels, K. N. Kudin, M. C. Strain, O. Farkas, J. Tomasi, V. Barone, M. Cossi, R. Cammi, B. Mennucci, C. Pomelli, C. Adamo, S. Clifford, J. Ochterski, G. A. Petersson, P. Y. Ayala, Q. Cui, K. Morokuma, D. K. Malick, A. D. Rabuck, K. Raghavachari, J. B. Foresman, J. Cioslowski, J. V. Ortiz, B. B. Stefanov, G. Liu, A. Liashenko, P. Piskorz, I. Komaromi, R. Gomperts, R. L. Martin, D. J. Fox, T. Keith, M. A. Al-Laham, C. Y. Peng, A. Nanayakkara, C. Gonzalez, M. Challacombe, P. M. W. Gill, B. Johnson, W. Chen, M. W. Wong, J. L. Andres, C. Gonzalez, M. Head-Gordon, E. S. Replogle, and J. A. Pople, *Gaussian 98, Revision* **A3**, Gaussian, Inc., Pittsburgh PA (1998).
34. G. Herzberg, *Spectra of Diatomic Molecules*, Van Nostrand Reinhold Co.: NY (1950).
35. B. Silvi, R. Wieczorek, Z. Latajka, M. E. Alikhani, A. Dkhissi, and Y. Bouteiller, *J. Chem. Phys.* **111**, 6671 (1999).
36. Y. Zhang, C-Y. Zhao, and X. Z. You, *J. Phys. Chem.* **A101**, 2879 (1997).
37. G. C. Pimentel and A. L. McCellar, *The Hydrogen Bond*, W. H. Freeman (ed.) San Francisco (1960).
38. A. C. Legon, *Chem. Soc. Rev.* **22**, 153 (1993).
39. K. R. Leopold, G. T. Fraser, S. E. Novick, and W. Kleperer, *Chem. Rev.* **94**, 1807 (1994).
40. H. M. McConnel, *J. Chem. Phys.* **29**, 1422 (1958).
41. C. K. Jen, *Electron spin resonance of trapped radicals, in: Formation and trapping of free radicals*, A. M. Bass and H. P. Broida (eds.), Academic, New York (1960).
42. L. Pauling, *Phys. Rev.* **36**, 430 (1930).
43. A. F. Devonshire, *Proc. Roy. Soc.* **A153**, 601 (1936).